THE EFFECTS OF GRAVITY ON THE MORPHOLOGY AND MORPHOMETRY OF EJECTA AND SECONDARY CRATERS ON THE MOON AND MERCURY.

K.R. Ramsley[1,2], [1]School of Engineering, Brown University, Box D, Providence, RI, USA. [2]Department of Geological Sciences, Brown University, Box 1846, Providence, RI, USA. (Kenneth_Ramsley@brown.edu)

Introduction: When comparing secondary impact features of Mercury to those of the Moon morphometric differences are observed in the distribution and character of primary impact ejecta These differences include 1) continuous ejecta deposition on Mercury that transition to distinct impact craters distally closer to the rims of primary craters, 2) typically tighter spatial emplacement densities of secondary craters on Mercury, 3) a proportionately wider range of secondary impact crater diameters on Mercury and 4) secondary craters on Mercury that are often proportionately larger and more uniformly circular. [1, 2, 3, 4, 5].

This study applies a reference template of secondary impact patterns to compare the influence of gravitation in the formation of secondary impact features on the Moon and on Mercury and suggests additional applications of this methodology.

Technique and Analysis Method: Observational templates are ideal patterns that are applied as filters to recorded data. For example, Bouguer anomalies are applied as filters to remove a known pattern of terrain elevations. The resulting dataset then describes variations from a well-characterized dataset that may reveal underlying factors [6]. In our study, under each planetary gravitation field, templates are defined that would result from ideal secondary emplacement processes. Templates of ideal secondary impact emplacement features provide a reference standard that reveals the extent of both significant and subtle morphometric differences between the Moon and Mercury. Templates may also facilitate comparisons of morphometric differences among similarly scaled secondary impact features on the same planetary body that result from factors other than gravitation.

Our method is based on the standard model of ejecta launch parameters [7 & 8]. For an initial test we have designed a set of approximately 500 Keplerian flight trajectories of ejecta fragments that would be produced during the formation of a 100 km diameter crater on a rocky terrestrial planet. Individual trajectories are derived from a timeline of launch events for the two principal types of ejecta that produce secondary impacts (spallation and excavation). Each ejecta test fragment is placed on the timeline according to five time-dependent event parameters, which are: 1) the radial rate of transient crater growth that defines the fragment launch site distance from the center of the primary crater, 2) the percentile of cumulative ejecta volume launched that defines the volume of ejecta at a given point on the timeline, 3) the ejection elevation angle for each fragment, 4) the ejection velocity for each fragment and 5) the fragment size. Zero seconds on the ejection timeline corresponds to the moment of impactor contact with the target; 68 seconds corresponds to the maximum radial extent of transient crater formation. **Figure 1** shows one of these parameters (excavation launch velocity).

We apply the same ejection timeline to both the Moon and Mercury by varying only the gravitational parameter GM and the spherical radius of the two bodies. In both simulations the same test fragments are ejected with exactly the same set of initial flight vectors and at the same points along the timeline. The only differences in the resulting patterns of secondary impacts are due to planetary gravitation and, to a lesser extent, planetary radius.

From each simulated flight we record: 1) secondary impact crater locations, 2) impact angles [same as the launch elevation], 3) estimated crater size and character, 4) flight durations and 5) peak flight altitudes. From these impact records we construct and plot results from a *terminal* timeline that is referenced to the arrival times of secondary impacts. Test trajectories are first computed for Mercury. Then, altering only the parameters of gravitation and spherical planetary radius, we rerun the test for the Moon. We overlay and compare simulated patterns of secondary impacts to examples of secondary impact patterns associated with 100-km-class craters on Mercury and on the Moon.

These comparisons allow us to: 1) assess how an ideal secondary impact emplacement process plays out sequentially as a dynamic process, 2) assess the extent to which identical datasets of ideal ejection vectors play out differently on each planetary body, 3) identify and map the obvious and subtle discrepancies in character where planetary features are inconsistent with the predictions of an ideal secondary impact pattern.

Results: When comparing our test simulations to the selected secondary impact features on Mercury and on the Moon, we observe the significant role that the greater gravitation of Mercury plays [1]. Specifically, our simulations confirm that the stronger gravitation of Mercury: 1) accounts for higher secondary impact spatial densities due to shorter downrange flights of ejecta, 2) strongly implies a proportionately closer distal radius of continuous ejecta deposition and closer proximity of distinct secondary craters surrounding primary craters, 3) confirms that ejecta trajectories on Mercury are more likely to emplace circular impact features due to the greater proportion of higher-velocity secondary impacts that fall closer to primary craters and 4) reveals that the Moon is exposed to approximately 20% to 30% fewer secondary impacts from the same test event due to lower lunar gravity which permits a larger portion of lunar ejecta to escape into space (**Fig 1**).

Discussion and Implications: Simulated patterns of ejecta predict differences of secondary ejecta patterns due to gravitational differences of the Moon and Mercury. This, however, does not account for differences in the character of ejecta emplacement patterns on the same planetary body that result from events of similar magnitude. Through the application of an ideal template pattern, we may compare ejecta patterns among craters of similar sizes on the same body to a fixed reference in order to characterize obvious and subtle deviations in character.

For example, the distribution of secondary impacts features that surround two similar craters on the same planet may appear nearly identical in spatial density, yet the distribution pattern of secondary impacts may deviate subtly. To assess these differences, areas of deviation in character may be observed in newly acquired data from the MESSENGER spacecraft to assess differences of substrate characteristics in greater detail [9].

Since gravity is nearly identical planet-wide on each body, the observed differences of morphometry among craters of similar ages and sizes are due solely to other factors. These factors may include impact velocity, local crustal coherence/strength due to volcanic intercrater and smooth plains, and impactor composition. For example, the range of potential impact velocities at Mercury is significant. These velocities vary from 15 to 80 km/s with a mean of 30 km/s [10], whereas the Earth/Moon system is typically exposed to impact velocities of 10 to 50 km/s with a mean of 20 km/s [11]. The wider range of potential impact velocities on Mercury (65 km/s versus 40 km/s at the Moon) may account for wider morphometric differences among similarly sized craters on Mercury. As the morphometry of higher-velocity impacts is better understood, templates may then be designed that select for narrow ranges of impact velocity patterns and may be used to gauge impact velocities.

Conclusions: The gravitational differences between the Moon and Mercury are sufficient to account for significant morphometric differences of secondary impact patterns when comparing the two planets. The subtle differences in the character of secondary impact patterns from craters of similar size on the same planetary body may be assessed by comparison with a fixed template that represents ideal patterns of ejecta distribution.

References:

[1] Gault, D. E., J. E. Guest, J. B. Murray, D. Dzurisin, and M. C. Malin, (1975), Some comparisons of impact craters on Mercury and the Moon, *J. Geophys. Res., 80(17)*, 2444–2460. [2] Melosh, H. J., (2008), Planetary science: Message from Mercury, *Nature 452*, 820-821. [3] Oberbeck, V. R., Morrison, R.H., and Hörz, F. (1975), Transport and emplacement of crater and basin deposits, *Earth, Moon, and Planets 13*, 9-26. [4] Schultz, P.H., and J. Singer (1980), A comparison of secondary craters on the Moon, Mercury and Mars, *Proc.Lunar Planet. Sci. Conf. 11th*, 2243-2259. [5] Cintala, M. L. and Grieve, A.F., (1998), Scaling impact melting dimensions: Implications for the lunar cratering record, *Meteorit. Planet. Sci., 889-912.* [6] Xiaohong, Lianghhui, Zhaoxi, Shuling and Lei, (2009), A method for gravity anomaly separation based on preferential continuation and its application, *Appl. Geophys. 6*, 217-225. [7] Melosh, H. J., (1989), Impact Cratering: A Geologic Process, *Oxford Univ. Press.* [8] Richardson, J. E., (2009), Modeling impact ejecta plume evolution: A comparison to laboratory studies, *J. Geophys. R*es. 116, 1-16. [9] Denevi, B. W., M. S. Robinson, S. C. Solomon, S. L. Murchie, D. T. Blewett, D. L. Domingue, T. J. McCoy, C. M. Ernst, J. W. Head III, T. R. Watters, and N. L. Chabot (2009), The evolution of Mercury's crust: A global perspective from MESSENGER, *Science, 324,* 613-618. [10] Minton, D. A. and Malhotra, R., (2010), Dynamical erosion of the asteroid belt and implications for large impacts in the inner solar system, *Icarus, 207*, 744-757. [11] Marchi , S., Morbidelli, A., Cremonese, G., (2005), Flux of meteoroid impacts on Mercury, *Astron. Astrophys.* 431, 1123-1127.

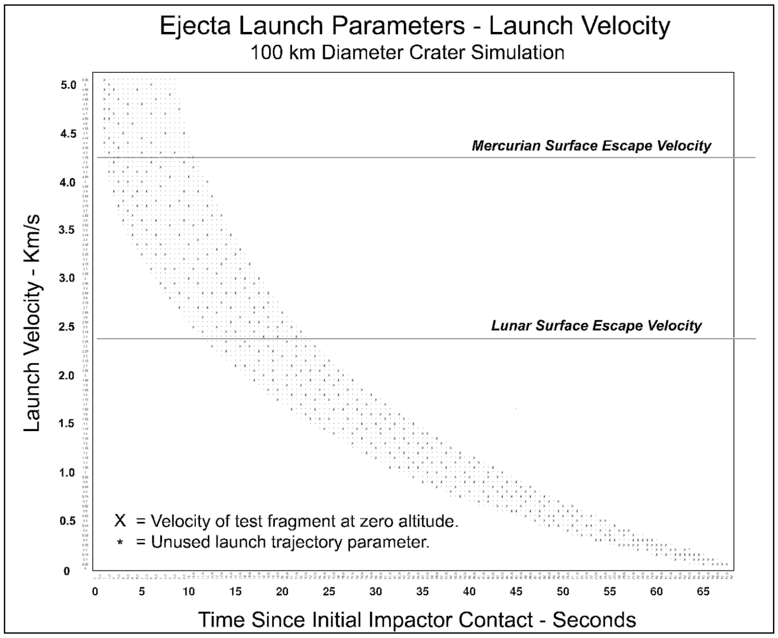

Figure 1 simulates a plausible timeline for the launch velocity of ejecta from a 100 km diameter crater formed by an impactor arriving at ~20 km/s. After ejection from the primary crater, fewer ejecta fragments would return to the surface of the Moon than to the surface of Mercury.